Electronic transport regimes through an alkoxythiolated diphenyl-2,2′-bithiophene-based molecular junction diodes: critical assessment of the thermal dependence†

Giuseppina Pace,*[a] Lorenzo Caranzi,[a,b] Sadir G. Bucella,[a,b] Eleonora V. Canesi,[c] Giorgio Dell'Erba,[a,d] Chiara Bertarelli[c] and Mario Caironi*[a]

Received 4th September 2014,
Accepted 9th November 2014

Introduction

The wide flexibility in tailoring the optoelectronic properties of organic materials has justified the efforts for integrating them into electronic circuits for technology application. Molecular electronics studies are motivated by the potential for future electronics being based on single molecules or ensembles of molecules, providing one possible answer for the extreme downscaling requirements needed to satisfy the ever increasing demand for a denser computational capability.[1] Self-assembly of functional molecules and their tunable chemical composition may also offer a means to deploy complex logic functionalities at the nanometer scale, through a unique and efficient bottom-up approach, thus enabling alternative applications not accessible with current technologies.[2] In order to achieve these targets, the fundamental properties of molecular junctions have to be investigated. Most of the current studies have focused on conductive atomic force microscopy (c-AFM) measurements[3,4] and the break junction approach.[5] These junction configurations enable very important fundamental studies, but they are still far from being suitable for the

[a]*Center for Nano Science and Technology@PoliMi, Istituto Italiano di Tecnologia, Via Pascoli 70/3, 20133 Milano, Italy. E-mail: giuseppina.pace@iit.it, mario.caironi@iit.it*

[b]*Dipartimento di Fisica, Politecnico di Milano, P.za L. Da Vinci, 32 20133 Milano, Italy*

[c]*Dipartimento di Chimica, Materiali e Ing. Chimica, Politecnico di Milano, P.za L. Da Vinci, 32 20133 Milano, Italy*

[d]*Dipartimento di Elettronica, Informazione e Bioingegneria, Politecnico di Milano, P.za L. Da Vinci, 32 20133 Milano, Italy*

†Electronic supplementary information (ESI) available. See DOI: 10.1039/c4nr05142d

following step of integration into a scaled-up technology. Furthermore, the transport properties so far investigated with the break junction technique are strongly correlated to the particular atomic configuration of the apex metal contacts, and the effectiveness in controlling the alignment of a single molecule between them. A more scalable design is based on ensemble molecular junction diodes, where many self-assembled molecules are sandwiched between two electrodes.[6] Various examples of ensemble molecular junctions can be found in the literature, and most of them exploit the self-assembling properties of thiolated molecules bound to gold electrodes.[6b] Typical artifacts encountered in the electrical characterization of molecular junctions are caused by metal diffusion filaments formed during the thermal evaporation of the top metal contact.[7] Unfortunately, the electronic conductivity of those filaments has been often misinterpreted and assigned to molecular charge transport features.[8] More recent strategies foresee the development of soft electrode deposition methods.[9] A valuable approach is the insertion of a protective poly(3,4-ethylenedioxythiophene)poly(styrenesulfonate) (PEDOT:PSS), acting as a conductive interlayer, between the self-assembled monolayer (SAM) and the thermally evaporated top metal contact.[10] Other research studies have also shown the effectiveness of using graphene and graphene oxides as soft contacts.[11] Once the diode configuration is defined, the junction transport properties have to be rationalized in light of the specific adopted architecture, and molecular features have to be extrapolated.

The typical transport mechanisms often found in a molecular junction are tunneling and resonant transport.[12] A non-resonant tunneling mechanism, which is temperature independent, is favored in the case of very thin monolayer and high energy offset between molecular orbital energy and electrode work function. Resonant transport mostly occurs when the molecule's Highest Occupied Molecular Orbital (HOMO) and Lowest Unoccupied Molecular Orbital (LUMO) are involved in the electronic transport through the electrode–molecule electronic coupling. In particular, the charge hopping mechanism operates under resonant conditions and features an Arrhenius dependence of the conductivity *versus* temperature. Non-resonant tunneling has been previously found to dominate for chain lengths shorter than 2.5 nm even for fully conjugated molecular wires.[13] For these molecules a hopping mechanism is more likely to occur when the chain length is longer than 5 nm.[14] So far, it has not been clear whether a hopping mechanism can be achieved for short and not fully conjugated systems.

In this work we present ensemble molecular junctions based on an alkoxythiolated 3,3′-diphenyl-2,2′-bithiophene (DPBT), which is designed to embed insulating alkyl chains in between the electrodes and the aromatic core. Multiple techniques have been employed in this study to unveil a molecular fingerprint in the electrical conduction, namely the robustness of the electrical parameters extracted with different junction architectures comprising the same DPBT molecule. In particular, c-AFM allows for an easier fabrication and a wider junction statistic with respect to pore-junctions. Therefore, our study foresees the use of c-AFM as a first technique which allows us to identify from the current–voltage (*I–V*) measurements a precise transition voltage (V_T), which is found as a minimum in the transition voltage plot, where the usual *I–V* data are plotted in a Fowler Nordheim (FN) manner (*i.e.*, $\ln(I/V^2)$ *vs.* $1/V$).[15]

The study then moves to the *I–V* characterization of a large number of micro-pore junctions with and without the PEDOT:PSS soft-contact. In both cases we found the same V_T as for c-AFM measurements, highlighting the critical role of the molecule in determining the junction transport characteristics independently from the top contact. Variable temperature *I–V* curves acquired on micro-pore junctions allow the proper investigation of the transport mechanism. Importantly, we were able to evidence clear agreement between variable temperature measurements on pore junctions with both top Au and PEDOT:PSS contacts. This is a critical finding, further confirming the specific role of the molecule in determining charge transport. Therefore, by combining different characterization techniques and by a critical assessment of the thermal dependence of the current–voltage (*I–V*) characteristic curves, we found that resonant transport can be achieved also for such short and not fully conjugated chains. We show that by a proper design of the highly occupied molecular orbital (HOMO) level, being very close to the gold work function, and by inserting a short insulating alkyl chain between the metal and the aromatic core, we could enable a thermally activated transport regime at low biases and at room temperature implying the contribution of the conjugated core of the molecule.

Results

The molecule under study (DPBT, Fig. 1) has an aromatic core and two insulating saturated alkyl chains constituted by six

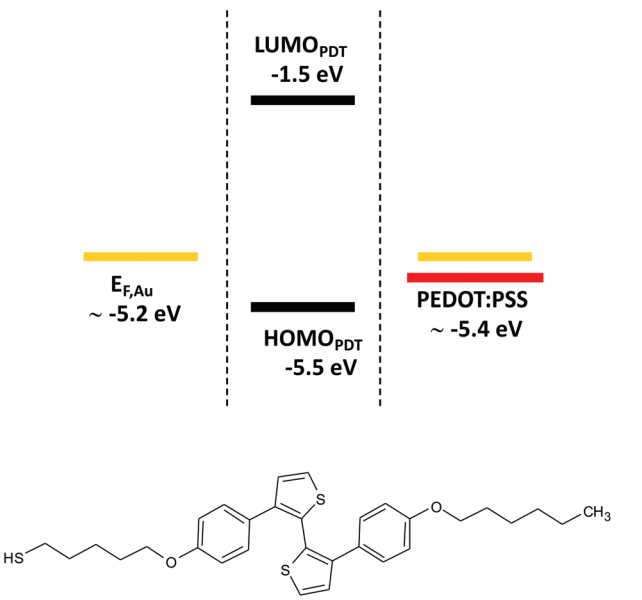

Fig. 1 Bottom: Molecular structure of 3-(4-hexyloxyphenyl)-3′-(4-(6-mercapto)hexyloxyphenyl)-2,2′-bithiophene (DPBT). Top: Scheme of energy levels.

carbon atoms, one of which terminated with a thiol group. The aromatic core determines its HOMO and LUMO, whose energies have been measured by cyclic voltammetry (CV, Fig. S1, ESI†). A DPBT monolayer was grown on a gold surface thanks to its anchoring –SH group, according to the methodology reported in the Methods section, and its presence was shown by grazing angle incidence reflection absorption infrared spectroscopy (RAIRS) data (Fig. S2 and Table 1 in ESI†).

We first investigated the conduction through such a monolayer by means of the c-AFM technique, *i.e.* by adopting the conductive tip of an AFM as the counter probing electrode.

I–V measurements were performed at room temperature and under a N_2 atmosphere. The collected data are reported in Fig. 2A and C, and compare c-AFM junctions containing saturated tetradecanethiol (C14) SAMs or DPBT SAMs chemisorbed on gold. C14 based junctions have been selected as reference samples since the C14 chain length is comparable to the DPBT one. Per molecule at least four freshly made SAM samples were characterized. Per SAM at least three different sampling points were tested. The data presented are averaged over at least 20 *I–V* curves acquired per tip load per testing point (raw data shown in Fig. S3†). We also present the data as a function of the applied load.[16] The lowest currents are measured by applying the minimum load necessary to make the first electrical contact to the SAM. For DPBT the higher load is the one preceding the SAM rupture, favoring a short circuit through the junction. As shown in Fig. 2, for similar tip loads the current intensities measured on C14 and DPBT (58 nN and 50 nN respectively) can be very different. Such differences may arise from a combined effect of different intrinsic conductivities and different mechanical properties of the two investigated SAMs due to the different packing and moisture adlayer, which affects the effective load to be applied for establishing the electrical contact to the SAM.

Though it has raised some controversy with respect to its proper interpretation, a useful tool to monitor the electrical characteristics of molecular junctions is the extrapolation of the transition voltage V_T from the FN plot derived from the *I–V* characteristics.[15,17] The theoretical concept behind this plot is the Simmons model,[18] which identifies in the V_T the voltage threshold for the transition between a direct tunneling and a Fowler Nordheim tunneling. However, care must be taken when assigning the minimum found in the V_T plot to either a transition between these or other specific mechanisms.[19,20]

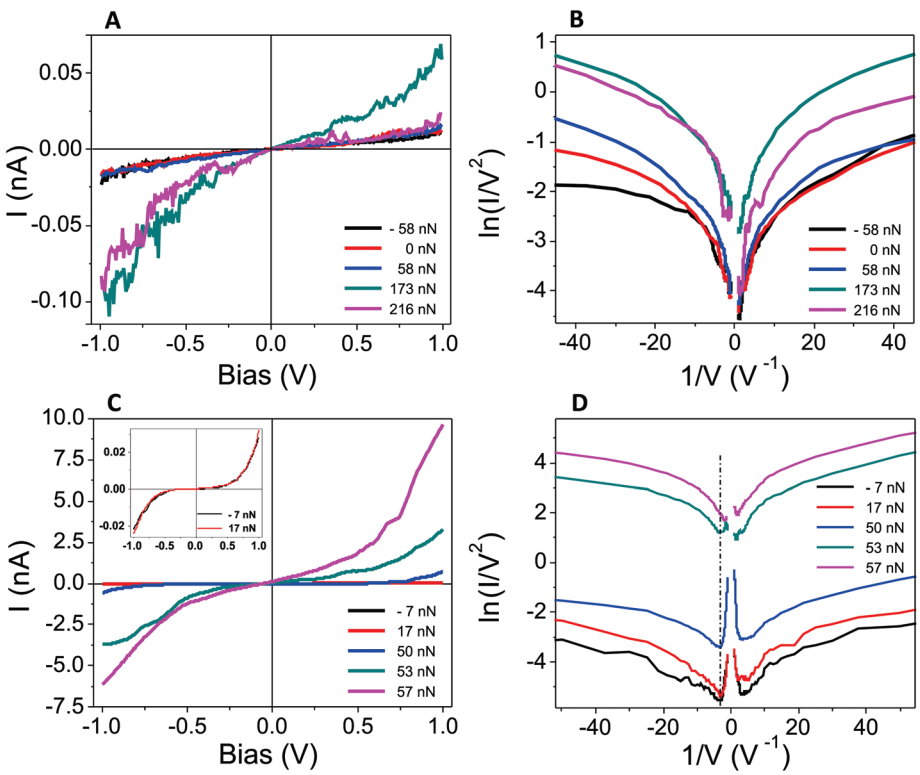

Fig. 2 *I–V* plot (A) and transition voltage plot (B) acquired on a c-AFM junction configuration for C14 SAM on gold; *I–V* plot (C) and transition voltage plot (D) acquired on a c-AFM junction configuration for DPBT SAM on gold. The inset in (C) shows the *I–V* plot acquired for the lowest applied tip loads. Lower loads correspond to the minimum load required to achieve an electrical contact with the SAM/Au substrate. At higher loads, short circuits are very likely to occur, producing increased current densities especially in the case of non-densely packed monolayers. However, in densely packed and insulating SAMs, as for the C14 SAM, increasing the tip-load implies a higher probability to contaminate the metallic tip with detachment and physisorption of the SAM molecules on the tip. Such cases can lead to the formation of a more insulating tip at increasing load with a consequent decrease of the measured current as we can see by comparing the *I–V* curve acquired for C14 SAM at 173 nN and 216 nN. The abrupt jump in conductance observed for C14 (above 58 nN) and for DPBT (above 53 nN) is likely associated with a tip breaking the SAM packing, thus reducing the gold substrate–tip distance, resulting also in a clear modification of V_T.

Vilan and Cahen analyzed different tunneling transport models and have shown that such minima can also be found when a Taylor expansion is used to introduce a small perturbation on a single tunneling mechanism, and therefore no transition between two different transport mechanisms would be needed to observe a V_T.[21]

Keeping in mind all the above, the *I–V* data measured for molecular junctions in a c-AFM configuration are presented for comparison, also in the form of transition voltage plots (Fig. 2B and D). By comparing the *I–V* curves for both DPBT and C14 samples at very low applied loads, where the current intensity measured for the two junctions is similar, we can clearly see that a V_T (~0.35 V) appears only for the DPBT SAM, while it is absent for the C14 one. Interestingly, the measured V_T for the DPBT junction is even lower than that found for very short alkyl chains, as for example for an octanethiol (C8) SAM, where a V_T of ~0.5 V was reported for high tip loads.[22] Also we observed that a persistent V_T is found for the entire range of applied loads for DPBT, contrary to the C14 SAM. With increasing the tip-load, V_T for DPBT stays almost constant at around $V_T = (0.32 \pm 0.03)$ V, while a jump to higher values occurs only for a tip-load closer to short circuit conditions of the diode (~0.5 V at 57 nN). From such an analysis we observe that, besides showing a higher conductivity (Fig. 2), DPBT junctions display a V_T which cannot be reproduced with a saturated carbon chain of similar and even shorter lengths. It is worth here to underline that our measurements on the reference C14 samples are consistent with previous reports on long alkyl chains, showing a V_T higher than 1 V,[23] at the limit of our bias window. Within this window we could observe a V_T at around ~0.7 V only for high tip loads and only for a few (10%) C14 junctions. Such a decrease in V_T was previously shown for alkanethiols and assigned to a different tilting angle of the alkyl chains with respect to the substrate, thus enabling different pathways for the charges to tunnel through the SAM.[22] This behavior is highly reproducible and implies that in c-AFM the applied tip load can play a major role in determining the transport properties of a junction, reflected by the overall current density and V_T.[16]

We then compared the c-AFM junction characteristics with those found in pore junction diode configurations. A sketch of all the three different diode configurations investigated in this study is shown in Fig. 3: (a) Au//DPBT//Au; (b) Au//DPBT/PEDOT:PSS//Au; (c) Au//DPBT//(Pt, c-AFM tip). Here, we would like to point out that the data presented are the outcome of over a thousand investigated pore junctions with and without the soft PEDOT:PSS electrode. In spite of the very low yield in fabricating the Au//DPBT//Au diode junction (~3%), due to the easy formation of short circuiting filaments, we could consistently and reproducibly compare those junctions with the Au//DPBT-PEDOT:PSS//Au diodes. As shown in Fig. 3, these data are also comparable with what was observed in a c-AFM diode configuration, where the top electrode is a conductive Pt coated tip. The analysis of the V_T plot, shown in Fig. 3, reveals that the normalized data are essentially the same. Interestingly, despite the differences in the investigation methods

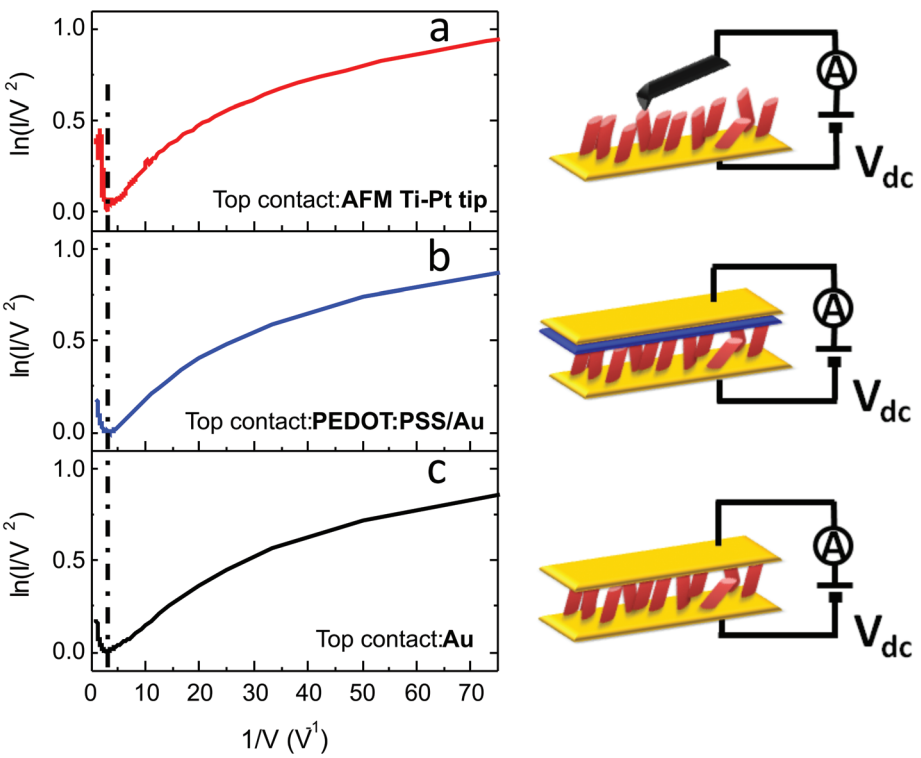

Fig. 3 Transition voltage plot of the measured *I–V* characteristics in the three diode configurations. (a) c-AFM junction, (b) PEDOT:PSS diode junction, and (c) Au junction. The dashed line is a guide to the eye showing the position of V_T.

employed, we found the same $V_T = (0.32 \pm 0.03)$ V all across the different approaches. Such V_T is therefore the fingerprint of the DPBT molecule in the conduction, no matter which junction configuration is used for the investigation. This appears as a first confirmation that the molecule rather than the diode structure is determining the junction's electrical properties. Such solid persistency of an electrical parameter associated with a conjugated molecular *ensemble* probed in different junction architectures has not been previously reported. Moreover, while the current density is usually not comparable in nano- and micro-pore junctions,[12a] as very often observed the current density does not scale with the junction area. The robustness of V_T for DPBT junctions highlights a possible discriminating factor when comparing junctions characterized by very different probing areas. As discussed above, a question arises about the possible physical origin of this parameter, V_T, in the junctions under investigation. This V_T corresponds to a clear change in conductivity of the junction, as shown by dI/dV measurements on a Au//DPBT//Au sample, directly performed with a lock-in based technique (see ESI,† Fig. S3). However at this stage we still cannot attribute the presence of a V_T to a transition between different transport mechanisms.

Deeper insights into the transport mechanism deserve further investigations. A molecular length dependence study is in principle an important tool to rationalize the transport regimes,[12a] as an exponential dependence of the conductivity on length would be compatible with a non-resonant tunneling process, while a linear dependence would imply an incoherent hopping process. However DPBT offers too many possibilities for varying the molecular length, as by changing the repeating unit in the aromatic core or in the alkylic side chains, making the approach not readily viable in this case. Temperature dependent measurements at different bias voltages become therefore mandatory to clearly disentangle and address different possible transport mechanisms.

Temperature and bias dependent measurements for the Au//DPBT//Au junction are shown in Fig. 4. Reversible, upward and downward temperature cycles demonstrate the stability of the junction. An analogous analysis performed on the thermal dependence of Au//DPBT-PEDOT:PSS//Au junctions (Fig. 5) allows for the same conclusions and observations (see the Discussion section). Independently of the underlying transport process, the substantial correspondence of the thermal dependence as found in junctions with and without PEDOT:PSS is a

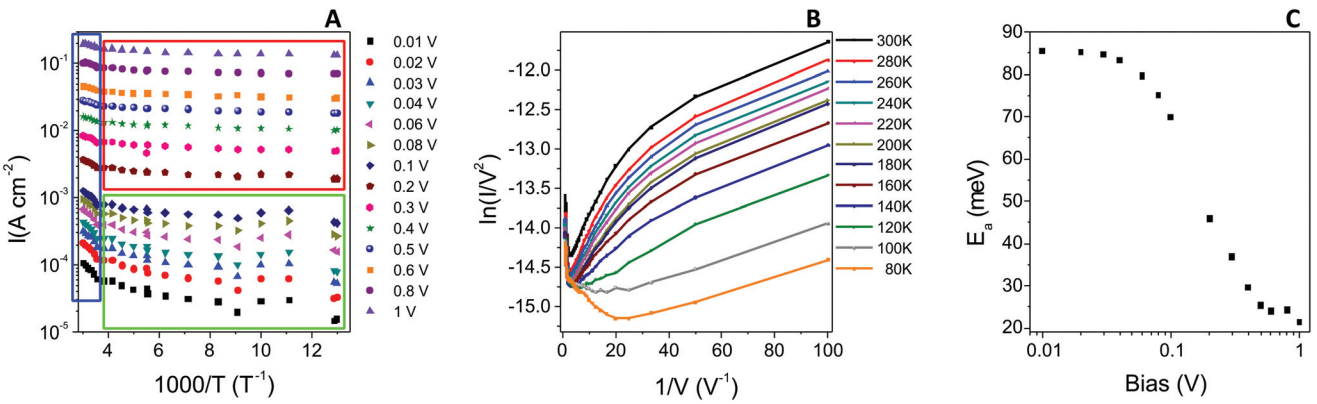

Fig. 4 (A) Current dependence on temperature and bias for a Au–DPBT–Au junction (reversible up-down cycles at 180 K and 77 K show the stability of the measured junction); (B) broadening of the transition voltage plot at lower temperatures (Au–DPBT–Au); (C) bias dependence of the activation energy as extracted from the Arrhenius plot of the current *vs.* temperature (T) for 330 < T < 280.

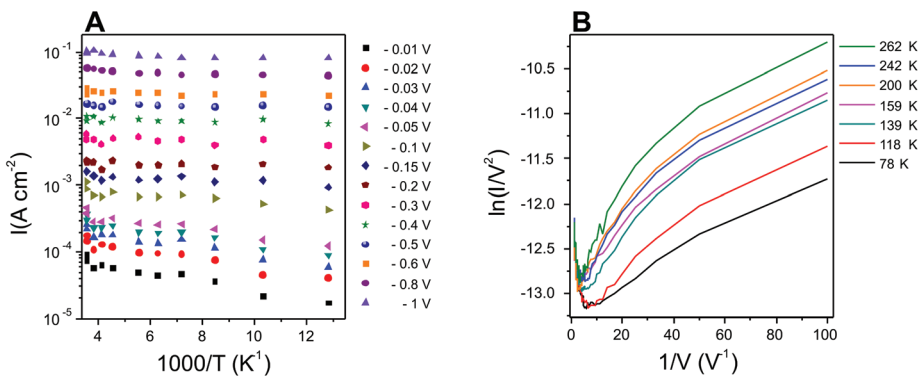

Fig. 5 (A) Current dependence on temperature and bias for a Au–DPBT–PEDOT:PSS–Au junction. (B) Transition voltage plot for a Au–DPBT–PEDOT:PSS–Au junction.

very critical evidence and confirms that the charge transport is not mainly ruled by the top conducting polymer or by defects following the deposition of the top Au electrode either, but is rather associated with a molecular contribution.

All the data shown in Fig. 4 are in the positive bias region and, due to the symmetry of the *I–V* curves at all temperatures, the same dependence is observed for the negative bias. Though this experimental evidence can be intuitive for the Au–SAM–Au sample, it is less straightforward to give a proper explanation for the observed symmetry in the PEDOT:PSS junctions. Similar findings have been previously reported for other molecular systems.[24] Possible causes for such a behavior are (i) the similar work functions of the two opposite electrodes, PEDOT:PSS and Au, providing the injection of similar current densities, or (ii) a Fermi level pinning regime.[25]

We also compared such a thermal dependence found for DPBT junctions with those spurious phenomena which can provide thermal dependent features even in saturated alkyl chain SAMs, and whose transport has been very often shown to be coherent and non-resonant. Such a comparative analysis is reported in the ESI,† and it shows that defective alkyl thiol junctions do not present the complex temperature dependence found for DPBT junctions.

Discussion

The temperature and bias dependent measurements of a Au//DPBT//Au junction are shown in Fig. 4A. The temperature dependence of the V_T is shown in Fig. 4B, where a broadening of the FN minima is observed at lower temperatures. For these junctions, a marked temperature dependence is observed in the temperature range between 330 and 280 K (blue box, Fig. 4A). A very weak or totally absent thermal dependence is expected in a non-resonant tunneling process, while a clear thermal activation has so far been rationalized either as an effect of contact Fermi level broadening within a non-resonant process or as a hopping process.[12a] We found that this data range can be fitted with an Arrhenius dependence, returning an activation energy (E_a) which is much higher at lower bias ($E_a \sim 85$ meV from 10 mV to 40 mV) and progressively decreases at higher biases (0.01–0.02 eV above 0.4 V, Fig. 4C). This proof strongly suggests that different mechanisms are responsible for the high bias and low bias regimes.

While the low bias and more strongly temperature dependent regime is discussed later,[26] for high bias and high temperature a good data fitting was found for a root square dependence of the current on temperature. Such a dependence has already been reported for injection processes at inorganic–organic interfaces and follows the Richardson–Schottky model for thermionic emission at a metal–vacuum interface.[27] This mechanism is very well in line with the bias independent activation energy found for higher biases (>0.4 V, Fig. 4C), *i.e.* biases higher than V_T.

From Fig. 4, at T below 280 K we can clearly recognize two regions as a function of the applied bias (indicatively, green and red boxes, Fig. 4A). Weak but measurable temperature dependence appears in the whole region from 280 K to 77 K at low biases, and an almost temperature independent region is found at higher biases. The temperature independent region above V_T can be easily assigned to a direct tunneling process which is field assisted (red box).[28]

A less straightforward assignment can be made for the ranges between 240–77 K and 10–50 mV (within the green box). A very good interpolation of those data is only found for a cubic dependence of the resistance on T (Fig. S5†). Such a dependence cannot be explained either with a purely molecular mechanism, a simple field assisted injection mechanism, or a thermionic emission. Such a power dependence on T is also responsible for the reversible broadening observed in the V_T plot (Fig. 4C). We highlight that this is very likely originating from the same mechanism responsible for a similar broadening already observed by Trouwborst *et al.*[29] for pure gold break junctions under vacuum conditions and in the absence of any molecular system. Therefore a molecular based mechanism cannot explain such a low temperature behavior. Here we provide a possible explanation for such a dependence. According to the Wiedemann–Franz law, relating the electrical conductivity with the thermal conductivity in metals, the presence of a temperature gradient between two electrodes, caused by the bias applied to one electrode, determines a power law dependence of the current *versus* temperature (see ESI† for the derivation). At the base of this power law is the current dependence on the metal phonon energy, *i.e.* on the role they play in the electron tunneling probability. While at room temperature all the metal phonons are already active, at low temperatures the activation of thermal phonons can increase the tunneling probability. So far the influence of the metal phonons on the electron transport processes in an organic diode studied at low temperatures has been disregarded, and molecular contributions to the transport have been claimed before considering such a spurious effect.[30] Hence, we propose that at very low bias and low temperature, thermal effects deriving from the metal electrode contacts can control the tunneling current. In conclusion, at temperatures below 280 K, the V_T which shifts to lower values (~0.32 V at 200 K and ~0.07 V at 80 K) is associated with a transition from a metal phonon mediated transport at low biases to a non-resonant tunneling transport at higher biases.

We discuss now the transport regime at low biases between 330 K and 280 K, where a marked temperature activation is found. An E_a of 85 meV is low when compared to the expected energy difference between the gold Fermi level and the HOMO of the molecule (~0.3 eV). According to a previously reported work, the calculated reorganization energy (λ) needed to ionize the DPBT aromatic unit under vacuum is $\lambda \sim$ (0.2–0.3) eV.[31] Considering the semi-classical Marcus model for electron transfer, which would imply a hopping process, E_a would be proportional to $\lambda/4$, which would make reasonable the low E_a value found from the slope in the Arrhenius plot. However, we cannot be conclusive at this stage regarding such a process, also considering that when the molecule is bound to a solid

substrate and interacts with nearest neighboring molecules in the SAM, the activation energy can be very different from what is calculated under vacuum for a single molecule and may not be simply associated with the molecular reorganization energy. Therefore other reasons for such a low energetic barrier have to be discussed first. Previous studies have already reported a similar activation energy (~0.1 eV), but mostly for fully conjugated systems embedded in a break junction[32] or in a c-AFM configuration.[33] Choi *et al.*[34] investigated a fully conjugated molecule, and according to their interpretation the observed low activation energy has to be assigned to the intramolecular hopping process, while no energetic barrier would exist at the gold–molecule interface. Similar conclusions were drawn by Luo *et al.*,[33] who embedded multiple units of a ruthenium complex within two alkylated side chains ($O–(CH_2)_6$). They showed similar low values for the activation energy, only when more than two ruthenium complexes were present, resulting in a very long molecular wire where a hopping process was more likely to occur. Sayed *et al.*[35] observed a very low activation energy (~0.1 eV) for a long and fully conjugated molecule in an all-carbon molecular junction. The discrepancy between this value and the expected hopping energy was explained in terms of the coherent tunneling process affected by a broadened Fermi function of the carbon electrode.[36] In particular, in order to explain their data, the authors introduced the thermal dependence of the Fermi function, as described by Simmons,[18,37] including molecular parameters such as the SAM dielectric constant and an electron effective mass dependent upon the molecular conjugation length. Besides the difficulty to associate an electron effective mass with the short conjugated molecules under study, we note that the Simmons model cannot explain the observed dependence of the activation energy from the bias observed in Fig. 4C. Therefore, the effect of the broadening of the Au Fermi function does not appear to be a strong enough argument for the observed temperature dependence in this case.[12b]

Therefore our observations of temperature activation at low bias can be rationalized with a hopping process. The fact that it appears only at low biases is consistent with the short length of the molecule, which is not long enough to effectively decrease the direct tunneling between the two electrodes. However, the same molecular length is not consistent with an intramolecular hopping process, *i.e.* with the presence of multiple hopping sites on the molecule. Therefore the only plausible explanation supporting hopping is that the aromatic core represents a single hopping site for the charge between the two electrodes. Further experiments will be needed to fully confirm this hypothesis, *e.g.* by varying the chain length of the alkylic spacers. We also notice that a pinning mechanism is also compatible with a hopping mechanism. The presence of the short insulating alkyl chains and the proximity of energy levels between the Fermi energy level of gold ($E_{F,gold}$) and the HOMO of DPBT could favor a metal–molecule coupling leading to molecular electron density redistributions. The formation of hybrid states, as also foreseen in the pinning mechanism, can also explain the observed low activation energy.[25,38]

Given the difficulty in assessing a tunneling mechanism according to the Simmons model, in all the other mechanisms described above both the molecules and the electrodes have to be considered to explain the observed data at low bias and close to room temperature, implying a resonant transport mechanism. In the literature, there are no clear reports of an electrode–molecule coupling despite the presence of insulating alkyl chains in short molecular wires.

Conclusions

A thorough comparison of various junctions' architectures demonstrates that the ubiquitous V_T = (0.32 ± 0.05) eV found for DPBT based junctions is a signature of the molecular role in charge transport. Temperature and bias dependent measurements allow the identification of different transport regimes. The substantial agreement between temperature dependent conduction in junctions with Au and PEDOT:PSS top electrodes rules out the possibility of trivial spurious effects (*e.g.* metal filaments) inducing such a temperature dependence. We showed that at low bias and close to ambient temperature a resonant transport (E_a = 85 meV) is possible for short and not fully conjugated molecules. This mechanism is compatible with the presence of a single localized state, strongly contributed by the aromatic core of the molecule, to which the charge injected from electrodes can hop to. In this frame, in agreement with recent studies on molecular junctions,[19a,21] we can exclude that for DPBT junctions V_T discriminates between direct and FN tunneling; instead, we show that for biases exceeding V_T and close to room temperature, a transition from a resonant to a thermionic emission takes place.[39]

In the low temperature range two other mechanisms are present. For biases exceeding V_T a thermal independent tunneling regime is clearly evidenced. Interestingly, at low temperatures and low biases, we found that thermal conductivity determines a power dependence of the current on temperature, though a tunneling mechanism is still occurring in the junction. We have associated such a regime with the influence of metal-phonons, a spurious, *i.e.* not involving molecular electronic levels, contribution to the junction transport.

While statistical measurements are, at present, one of the most reasonable approaches for studying molecular junctions, we would emphasize the importance of temperature dependence studies to gather more awareness of the multiple channels which might contribute to junction transport, in particular those non-molecular mechanisms which might mislead the interpretation.

The overall importance of our work relies on both highlighting the robustness of an electrical parameter such as V_T with respect to the variation in junction architecture and probing area, and the definition of the fundamental parameters, energy level proximity to the electrode work function and alkyl chain length, which can control the resonant trans-

port in molecular junctions with a conjugated core. Resonant processes are most desirable as they would bring in the particular signature of the chosen molecules, making worthwhile the specific effort into design and synthesis.

Methods

The ω-alkylthiol functionalized 3,3′-diphenyl 2,2′-bithiophene (DPBT) has been synthesized using a previously reported route.[40]

A scheme of the diode junction studied in this work is presented in Fig. 1. The diode junction has been prepared by vacuum evaporation of 70 nm of gold onto 1737F glass slides. A ~1.3 μm thick photoresist layer (S1813) was spun on the gold substrate. Subsequently, part of the photoresist was removed through a photolithographic process, providing a patterning with 5–10–20–40–80 μm diameter holes. After oxygen plasma treatment (100 W, 10 min), the substrates were immersed overnight in a 5×10^{-4} M solution of DPBT in toluene. After vigorous rinsing with chloroform and drying under N_2, the samples were either directly placed in the evaporator chamber for the gold top electrode deposition or topped with a PEDOT:PSS layer. In the last case, the PEDOT:PSS interlayer was deposited by spin-coating on top of the molecular assembly prior to gold electrode evaporation.

Variable temperature *I–V* measurements have been performed using an Agilent B1500 Semiconductor Parameter Analyzer in a cryogenic probe-station (Janis). The temperature value was monitored with 4 sensors placed in different position of the chamber. To allow for a good thermal contact between the heat exchanger and the sample, the substrate was attached to the sample holder through a thermal paste (ApiezonN). The temperature on the top surface of the sample was also monitored in control experiments by recording the temperature of an additional Si diode sensor placed on top of a dummy 1737F glass substrate of the same thickness and comparable lateral dimensions of the actual samples.

Direct measurements of the first derivative of the *I–V* curves were performed by providing a DC bias with a superimposed AC of 10 mV at 654 Hz through a Keithley 3390 signal generator and by reading the output AC signal at 654 Hz, amplified with a transimpedance amplifier (DHPCA-100, FEMTO Messtechnik GmbH), on a lock-in amplifier (SRS830, Stanford Research Systems). These measurements were performed at 77K.

I–V characteristics have also been measured on a DPBT SAM chemisorbed on a clean gold surface through a conductive probe atomic force microscope (c-AFM, 5500 Agilent Technology). The gold substrates used for c-AFM junction experiments were prepared by evaporating 1.5 nm of Cr on mica prior to the evaporation of a 20 nm thick layer of gold. This allows us to obtain the substrate with a roughness of ~1.5 nm. Conductive platinum-coated silicon nitride cantilevers (N9540-60002, Agilent Technologies, Santa Clara, CA) with a nominal force constant of 6 N m^{-1} were used for c-AFM measurements. Measurements were carried out under a nitrogen atmosphere. We observed that *I–V* characteristics measured with c-AFM are dependent upon the force constant of the chosen tip, with higher tip forces being responsible for SAM penetration and formation of short circuits.[41]

References

1 (*a*) H. Song, M. A. Reed and T. Lee, *Adv. Mater.*, 2011, **23**, 1583; (*b*) R. M. Metzger and D. L. Mattern, *Top. Curr. Chem.*, 2012, **313**, 39.

2 (*a*) G. Pace, V. Ferri, C. Grave, M. Elbing, C. von Hanisch, M. Zharnikov, M. Mayor, M. A. Rampi and P. Samori, *Proc. Natl. Acad. Sci. U. S. A.*, 2007, **104**, 9937; (*b*) G. Pace, A. Petitjean, M. N. Lalloz-Vogel, J. Harrowfield, J. M. Lehn and P. Samori, *Angew. Chem., Int. Ed.*, 2008, **47**, 2484.

3 J. M. Mativetsky, G. Pace, M. Elbing, M. A. Rampi, M. Mayor and P. Samori, *J. Am. Chem. Soc.*, 2008, **130**, 9192.

4 (*a*) S. Chang, J. He, P. M. Zhang, B. Gyarfas and S. Lindsay, *J. Am. Chem. Soc.*, 2011, **133**, 14267; (*b*) C. M. Guedon, H. Valkenier, T. Markussen, K. S. Thygesen, J. C. Hummelen and S. J. van der Molen, *Nat. Nanotechnol.*, 2012, **7**, 304; (*c*) S. V. Aradhya, M. Frei, M. S. Hybertsen and L. Venkataraman, *Nat. Mater.*, 2012, **11**, 872.

5 (*a*) M. L. Perrin, C. J. O. Verzijl, C. A. Martin, A. J. Shaikh, R. Eelkema, J. H. van Esch, J. M. van Ruitenbeek, J. M. Thijssen, H. S. J. van der Zant and D. Dulic, *Nat. Nanotechnol.*, 2013, **8**, 282; (*b*) M. A. Reed, C. Zhou, C. J. Muller, T. P. Burgin and J. M. Tour, *Science*, 1997, **278**, 252.

6 (*a*) C. Zhou, M. R. Deshpande, M. A. Reed, L. Jones and J. M. Tour, *Appl. Phys. Lett.*, 1997, **71**, 611; (*b*) S. Park, G. Wang, B. Cho, Y. Kim, S. Song, Y. Ji, M. H. Yoon and T. Lee, *Nat. Nanotechnol.*, 2012, **7**, 438.

7 Y. C. Yang, P. Gao, S. Gaba, T. Chang, X. Q. Pan and W. Lu, *Nat. Commun.*, 2012, **3**, 732.

8 A. J. Bergren, K. D. Harris, F. J. Deng and R. L. McCreery, *J. Phys.: Condens. Matter*, 2008, **20**, 374117.

9 (*a*) A. P. Bonifas and R. L. McCreery, *Nat. Nanotechnol.*, 2010, **5**, 612; (*b*) A. B. Neuhausen, A. Hosseini, J. A. Sulpizio, C. E. Chidsey and D. Goldhaber-Gordon, *ACS Nano*, 2012, **6**, 9920.

10 (*a*) H. B. Akkerman, R. C. G. Naber, B. Jongbloed, P. A. van Hal, P. W. M. Blom, D. M. de Leeuw and B. de Boer, *Proc. Natl. Acad. Sci. U. S. A.*, 2007, **104**, 11161; (*b*) A. B. Neuhausen, A. Hosseini, J. A. Sulpizio, C. E. D. Chidsey and D. Goldhaber-Gordon, *ACS Nano*, 2012, **6**, 9920.

11 (*a*) M. Min, S. Seo, S. M. Lee and H. Lee, *Adv. Mater.*, 2013, **25**, 7045; (*b*) S. Seo, M. Min, J. Lee, T. Lee, S. Y. Choi and H. Lee, *Angew. Chem., Int. Ed.*, 2012, **51**, 108.

12 (*a*) L. A. Luo, S. H. Choi and C. D. Frisbie, *Chem. Mater.*, 2011, **23**, 631; (*b*) S. Y. Sayed, J. A. Fereiro, H. J. Yan, R. L. McCreery and A. J. Bergren, *Proc. Natl. Acad.*

Sci. U. S. A., 2012, **109**, 11498; (*c*) R. L. McCreery, H. J. Yan and A. J. Bergren, *Phys. Chem. Chem. Phys.*, 2013, **15**, 1065.
13 R. L. McCreery, *Chem. Mater.*, 2004, **16**, 4477.
14 (*a*) S. H. Choi, B. Kim and C. D. Frisbie, *Science*, 2008, **320**, 1482; (*b*) T. Hines, I. Diez-Perez, J. Hihath, H. Liu, Z.-S. Wang, J. Zhao, G. Zhou, K. Mullen and N. Tao, *J. Am. Chem. Soc.*, 2010, **132**, 11658.
15 J. M. Beebe, B. Kim, C. D. Frisbie and J. G. Kushmerick, *ACS Nano*, 2008, **2**, 827.
16 V. B. Engelkes, J. M. Beebe and C. D. Frisbie, *J. Phys. Chem. B*, 2005, **109**, 16801.
17 J. M. Beebe, B. Kim, J. W. Gadzuk, C. D. Frisbie and J. G. Kushmerick, *Phys. Rev. Lett.*, 2006, **97**, 026801.
18 J. G. Simmons, *J. Appl. Phys.*, 1964, **35**, 2655.
19 (*a*) I. Baldea, *Chem. Phys.*, 2012, **400**, 65; (*b*) I. Bâldea, *RSC Adv.*, 2014, **4**, 33257.
20 J. M. T. Fatemeh Mirjani and S. J. van der Molen, *Phys. Rev. B: Condens. Matte*, 2011, **84**, 115402.
21 A. Vilan, D. Cahen and E. Kraisler, *ACS Nano*, 2013, **7**, 695.
22 G. Wang, T. W. Kim, G. Jo and T. Lee, *J. Am. Chem. Soc.*, 2009, **131**, 5980.
23 M. C. Lennartz, N. Atodiresei, V. Caciuc and S. Karthauser, *J. Phys. Chem. C*, 2011, **115**, 15025.
24 (*a*) A. J. Kronemeijer, I. Katsouras, E. H. Huisman, P. A. van Hal, T. C. T. Geuns, P. W. M. Blom and D. M. de Leeuw, *Small*, 2011, **7**, 1593; (*b*) A. J. Kronemeijer, H. B. Akkerman, T. Kudernac, B. J. van Wees, B. L. Feringa, P. W. M. Blom and B. de Boer, *Adv. Mater.*, 2008, **20**, 1467; (*c*) G. Wang, S. I. Na, T. W. Kim, Y. Kim, S. Park and T. Lee, *Org. Electron.*, 2012, **13**, 771.
25 (*a*) C. Van Dyck, V. Geskin and J. Cornil, *Adv. Funct. Mater.*, 2014, **24**, 6154; (*b*) S. Braun, W. R. Salaneck and M. Fahlman, *Adv. Mater.*, 2009, **21**, 1450.
26 J. H. Worne, J. E. Anthony and D. Natelson, *Appl. Phys. Lett.*, 2010, **96**.
27 J. C. Scott, *J. Vac. Sci. Technol., A*, 2003, **21**, 521.
28 (*a*) J. C. Scott and G. G. Malliaras, *Chem. Phys. Lett.*, 1999, **299**, 115; (*b*) T. N. Ng, W. R. Silveira and J. A. Marohn, *Phys. Rev. Lett.*, 2007, **98**, 066101.
29 M. L. Trouwborst, C. A. Martin, R. H. M. Smit, C. M. Guedon, T. A. Baart, S. J. van der Molen and J. M. van Ruitenbeek, *Nano Lett.*, 2011, **11**, 614.
30 K. Asadi, A. J. Kronemeijer, T. Cramer, L. J. A. Koster, P. W. M. Blom and D. M. de Leeuw, *Nat. Commun.*, 2013, **4**, 1710.
31 D. Fazzi, C. Castiglioni, F. Negri, C. Bertarelli, A. Famulari, S. V. Meille and G. Zerbi, *J. Phys. Chem. C*, 2008, **112**, 18628.
32 M. A. C. Yoram Selzer, T. S. Mayer and D. L. Allara, *J. Am. Chem. Soc.*, 2004, **126**, 4052.
33 L. Luo, A. Benameur, P. Brignou, S. H. Choi, S. Rigaut and C. D. Frisbie, *J. Phys. Chem. C*, 2011, **115**, 19955.
34 S. H. Choi, C. Risko, M. C. R. Delgado, B. Kim, J. L. Bredas and C. D. Frisbie, *J. Am. Chem. Soc.*, 2010, **132**, 4358.
35 A. B. Sayed Youssef Sayed, M. Kondratenko, Y. Leroux, P. Hapiot and R. L. McCreery, *J. Am. Chem. Soc.*, 2013, **135**, 12972.
36 H. J. Yan, A. J. Bergren, R. McCreery, M. L. Della Rocca, P. Martin, P. Lafarge and J. C. Lacroix, *Proc. Natl. Acad. Sci. U. S. A.*, 2013, **110**, 5326.
37 A. J. Bergren, R. L. McCreery, S. R. Stoyanov, S. Gusarov and A. Kovalenko, *J. Phys. Chem. C*, 2010, **114**, 15806.
38 G. Heimel, S. Duhm, I. Salzmann, A. Gerlach, A. Strozecka, J. Niederhausen, C. Burker, T. Hosokai, I. Fernandez-Torrente, G. Schulze, S. Winkler, A. Wilke, R. Schlesinger, J. Frisch, B. Broker, A. Vollmer, B. Detlefs, J. Pflaum, S. Kera, K. J. Franke, N. Ueno, J. I. Pascual, F. Schreiber and N. Koch, *Nat. Chem.*, 2013, **5**, 187.
39 (*a*) A. V. Pakoulev and V. Burtman, *J. Phys. Chem. C*, 2009, **113**, 21413; (*b*) J. C. Li, D. Wang and D. C. Ba, *J. Phys. Chem. C*, 2012, **116**, 10986.
40 E. V. Canesi and C. Bertarelli, *Phosphorus, Sulfur Silicon Relat. Elem.*, 2011, **186**, 1298.
41 (*a*) J. J. D. Jianwei Zhao, *Nanotechnology*, 2003, **14**, 1023; (*b*) D. J. W. C. D. Frisbie, *J. Am. Chem. Soc.*, 2001, **123**, 5549.